PLOS ONE

RESEARCH ARTICLE

New formulation of the Gompertz equation to describe the kinetics of untreated tumors

Antonio Rafael Selva Castañeda[1,2], Erick Ramírez Torres[3], Narciso Antonio Villar Goris[4,5,6], Maraelys Morales González[7], Juan Bory Reyes[8], Victoriano Gustavo Sierra González[9], María Schonbek[10], Juan Ignacio Montijano[1]*, Luis Enrique Bergues Cabrales[1,6]*

1 Departamento de Matemática Aplicada, Instituto Universitario de Matemáticas y Aplicaciones, Universidad de Zaragoza, Zaragoza, Spain, **2** Departamento de Telecomunicaciones, Facultad de Ingeniería en Telecomunicaciones Informática y Biomédica, Universidad de Oriente, Santiago de Cuba, Cuba, **3** Departamento de Biomédica, Facultad de Ingeniería en Telecomunicaciones Informática y Biomédica, Universidad de Oriente, Santiago de Cuba, Cuba, **4** Universidad Autónoma de Santo Domingo, Santo Domingo, Dominican Republic, **5** Universidad Católica Tecnológica del CIBAO, Ucateci, La Vega, Dominican Republic, **6** Departamento de Ciencia e Innovación, Centro Nacional de Electromagnetismo Aplicado, Universidad de Oriente, Santiago de Cuba, Cuba, **7** Departamento de Farmacia, Facultad de Ciencias Naturales y Exactas, Universidad de Oriente, Santiago de Cuba, Cuba, **8** ESIME-Zacatenco, Instituto Politécnico Nacional, CD-MX, Mexico, **9** Grupo de las Industrias Biotecnológica y Farmacéuticas (BioCubaFarma), La Habana, Cuba, **10** Department of Mathematics, University of California Santa Cruz, Santa Cruz, CA, United States of America

* monti@unizar.es(JIM); berguesc@yahoo.com(LEBC)

Citation: Castañeda ARS, Torres ER, Goris NAV, González MM, Reyes JB, González VGS, et al. (2019) New formulation of the Gompertz equation to describe the kinetics of untreated tumors. PLoS ONE 14(11): e0224978. https://doi.org/10.1371/journal.pone.0224978

Editor: Fabio Rapallo, Universita degli Studi di Genova, ITALY

Received: November 7, 2018

Accepted: October 26, 2019

Published: November 12, 2019

Data Availability Statement: All relevant data are within the paper and its Supporting Information files.

Funding: This work has been partially supported by the Oriente University, Cuba, under the grants #7227 and 7228, Cuba, and MINECO, Spain, under the Project MTM2016-77735-C3-1-P. The University of the East paid for the experiments. The funders had no role in study design, data collection and analysis, decision to publish, or preparation of the manuscript.

Abstract

Background

Different equations have been used to describe and understand the growth kinetics of undisturbed malignant solid tumors. The aim of this paper is to propose a new formulation of the Gompertz equation in terms of different parameters of a malignant tumor: the intrinsic growth rate, the deceleration factor, the apoptosis rate, the number of cells corresponding to the tumor latency time, and the fractal dimensions of the tumor and its contour.

Methods

Furthermore, different formulations of the Gompertz equation are used to fit experimental data of the Ehrlich and fibrosarcoma Sa-37 tumors that grow in male BALB/c/Cenp mice. The parameters of each equation are obtained from these fittings.

Results

The new formulation of the Gompertz equation reveals that the initial number of cancerous cells in the conventional Gompertz equation is not a constant but a variable that depends nonlinearly on time and the tumor deceleration factor. In turn, this deceleration factor depends on the apoptosis rate of tumor cells and the fractal dimensions of the tumor and its irregular contour.

Competing interests: The authors have declared that no competing interests exist.

Conclusions

It is concluded that this new formulation has two parameters that are directly estimated from the experiment, describes well the growth kinetics of unperturbed Ehrlich and fibrosarcoma Sa-37 tumors, and confirms the fractal origin of the Gompertz formulation and the fractal property of tumors.

Introduction

One of the most interesting problems of current oncology is the understanding of the growth kinetics of a malignant tumor, named TGK (TGK), which follows a sigmoidal law. The TGK analysis is equally made by means of graphs of the number of cancer cells (n) versus time t, named n(t); tumor volume (V) versus t, named V(t); and/or the tumor mass (m) versus t, named m(t). This is due to the close relationship between these three physical quantities. Additionally, the sigmoidal form of TGK has been described by different equations, such as Gompertz, Logistics, Bertalanffy-Richards, Kolmogorov-Johnson-Mehl-Avrami modified, being the Gompertz equation (GE) the most used [1–3].

Izquierdo-Kulich et al. [4] report the fractal origin of GE (see appendix A). This fractal origin has also been reported in [5–8] but in terms only of the fractal dimension D_f. Here, we have considered the one in [4] because it also takes into account the fractal structure of the boundary of the tumor.

In the different formulations of the GE [1–3] and in the experiment [9, 10] the starting point of TGK is considered when the initial number of tumor cells (n_0) and the initial tumor volume (V_0) satisfy the conditions n (t = 0) = n_0 and V (t = 0) = V_0, respectively. In preclinical studies, the researcher chooses n_0/V_0 depending on the purpose of the investigation. The time that elapses from the inoculation of the tumor cells in the host until the tumor reaches n_0/V_0 is named t_0 [1, 3, 9]. Nevertheless, in clinics, n_0/V_0 corresponds to the tumor detected for the first time by the doctor by means of clinical and/or imaging methods. For this case, t_0 is the time that elapses from the tumor formation in the organism (via chemical, biological and/or physical carcinogens) [10], until its detection for the first time. This supposes $n_0 \geq n_{med}$, where n_{med} is the minimum number of quantifiable cancer cells contained in the smallest measurable tumor volume, named V_{med} ($V_0 \geq V_{med}$). The post-inoculation time that elapses until the tumor reaches n_{med}/V_{med} is named t_{med} ($t_0 \geq t_{med}$) [3].

In [4], it is considered the Gompertz equation given in Eq (1) (named GE_1)

$$n(t) = e^{\left(\frac{\alpha}{\beta}\right)\left(1-e^{-\beta t}\right)}. \quad (1)$$

According the considerations in the previous paragraph, GE_1 has two limitations: 1) $n_0 = 1$, which means that the tumor has only one cell when it reaches V_0, in contradiction with the experiment [9, 10]. 2) The maximum capacity of the tumor (n_∞) depends only on α and β and not on n_0 ($n(t) = n_\infty = e^{\alpha/\beta}$ when $t \rightarrow \infty$). From the mathematical point of view, n_∞ is the upper asymptote of TGK. Nevertheless, in the preclinical, the condition $t \rightarrow \infty$ is the post-inoculation time that elapses until the tumor reaches a certain volume, for which animals are sacrificed for ethical reasons [1]. In clinics, this condition means the time that elapses from the tumor formation in the organism until the patient dies.

Each undisturbed solid tumor histological variety, that grows in a type of syngeneic host to it, has its own natural history (only sigmoidal law), which does not depend on the selection of

n_0/V_0, as observed in [3, 10–12]. In the experiment, once the researcher fixes n_0/V_0, t_0 can be estimated *a priori* when the tumor latency time is known, named t_{obs} ($t_{obs} < t_0$), which is the post-inoculation time that elapses until that the tumor is observed for the first time. In this case, the tumor is observable and palpable but not measurable. However, its size, named V_{obs} ($V(t = t_{obs}) = V_{obs}$), is estimated following the methodology reported in [1, 3]. When the tumor reaches V_{obs}, it contains a number of cells, named n_{obs} ($n(t = t_{obs}) = n_{obs}$).

The interest of including n_{obs}/V_{obs} ($n_{obs}/V_{obs} < n_{med}/V_{med} \leq n_0/V_0$) in GE is because an important part of vital cycle of a solid tumor occur before it is clinically detected (V_{med}), as reported in [1, 3, 10]. Furthermore, a high cellular viability ($\geq 95\%$) and a correct inoculation of the initial concentration of tumor cells (c_o) are guaranteed, t_{obs} can be known *a priori* for a tumor histological variety that grows in a certain type of syngeneic host to it [3, 9–11].

As far as we reviewed, few experimental works report the analysis of TGK from V_{obs} [1, 3] and none of equations used to describe TGK includes n_{obs}/V_{obs}. In addition, in the literature a relationship of α and β in terms of D_f, d_f and n_{obs}/V_{obs} has not been reported in the literature. Therefore, the aim of this paper is to propose a new formulation of the GE that includes n_{obs}/V_{obs}, n_0/V_0, α, β, and to study the relation of these parameters with the fractal dimensions D_f and d_f. The validity of this new mathematical formulation and the estimation of its parameters are determined from volumes of the Ehrlich and fibrosarcoma Sa-37 tumors that grow in BALB/c/Cenp mice, previously reported in [9]. Furthermore, the graphs of α versus d_f and β versus d_f/D_f for different values of u_2 (the constant of the velocity of apoptosis) and n_{obs} are shown.

Methods

Conventional Gompertz equation

Eq (2), named GE_2, is the conventional GE and the most used when TGK starts at n_0/V_0, given by

$$n(t) = n_0\, e^{\left(\frac{\alpha}{\beta}\right)(1-e^{-\beta t})}. \tag{2}$$

According to GE_2, n_∞ depends on n_0, α and β ($n(t) = n_\infty = n_0\, e^{\alpha/\beta}$ when $t \to \infty$) and results from solving the ordinary differential Eq (3) with its initial condition, given by

$$\begin{cases} \dfrac{dn}{dt} = \alpha n - \beta n \ln\dfrac{n}{n_0} = \alpha n\left(1 - \dfrac{\beta}{\alpha}\ln\dfrac{n}{n_0}\right) \\ n(t=0) = n_0 \end{cases}. \tag{3}$$

GE_2 suggests that n_0 (constant in time) has to be included in Eq (A2). Tjørve and Tjørve [2] report that n_0 acts as a parameter of shape (n_∞ changes with n_0) or location (n_∞ remains constant).

Inclusion of n_0 in Eq (A2)

In this topic was followed the methodology exposed in [4] and the initial number of tumor cells at t = 0, named n_{00}, was included in Eq (A2), resulting the following problem

$$\begin{cases} \dfrac{d\ln(n)}{dt} = u_2(\theta - 1)\ln\left(\dfrac{n}{n_{ss}}\right) \\ \ln(n)_{t=0} = \ln(n_{00}) \quad n(t=0) = n_{00} \end{cases}. \tag{4}$$

The exact solution of Eq (3) was given by

$$n(t) = (n_{00})^{e^{-\beta t}}\, e^{\left(\frac{\alpha}{\beta}\right)(1-e^{-\beta t})}, \tag{5}$$

with

$$\begin{cases} \alpha = u_2\left[\ln\dfrac{U_1}{u_2}\right] = u_2 \ln\left(\dfrac{\frac{2}{3}d_f - 1}{d_f - 1}\right) \\ \beta = u_2(1-\theta) = u_2\left(1 - \dfrac{d_f}{D_f}\right) \end{cases}. \tag{6}$$

Two inconsistencies were found in [4]: 1) the coefficient 1.5 in the parameter α of Eq (A3) was not correct but 2/3, as in Eq (6). 2) Different types of experimental tumors with the same values of d_f and D_f had different values of α/β (we refer to the reader see Table 1 of [4]), in contrast to Eq (A3).

Eq (5), named GE_5, agrees with GE_2 when $n_0 = (n_{00})^{e^{-\beta t}}$. In addition, the parameters n_{00} and n_0 coincided exactly at t = 0. The constant parameter n_{00} ($n_{00} \geq n_{med}$) constituted the starting point of TGK for GE_5 and reached for $t = t_0$. Therefore, it was convenient to

Table 1. Parameters of the models for the Ehrlich tumor.

Parameters	Different formulations of Gompertz equations			
	GE_1	GE_2	GE_5	GE_8
α ($days^{-1}$)	0.160±0.005	0.466±0.012	0.285±0.004	0.719±0.067
β ($days^{-1}$)	0.122±0.007	0.261±0.007	0.261±0.007	0.261±0.007
$V_{obs(\alpha,\beta)}$ (cm^3)	-	-	-	0.190±0.063
u_2 ($days^{-1}$)	0.263±0.066	0.633±0.141	0.391±0.055	0.687±0.131
d_f	0.720±0.061	0.768±0.056	0.764±0.032	0.611±0.052
D_f	1.467±0.410	1.404±0.346	1.583±0.836	1.023±0.192
$V_{obs(u2,df,Df)}$ (cm^3)	-	-	-	0.190±0.041
α_c ($days^{-1}$)	0.163±0.003	0.471±0.009	0.286±0.005	0.724±0.055
β_c ($days^{-1}$)	0.134±0.104	0.287±0.005	0.275±0.009	0.261±0.007
SE	0.215±0.006	0.884±0.021	0.088±0.021	0.089±0.021
PRESS	1.313±0.154	0.015±0.012	0.015±0.012	0.016±0.012
MPRESS	1.128±0.144	0.015±0.012	0.015±0.012	0.016±0.012
r^2	0.990±0.006	0.998±0.009	0.998±0.009	0.998±0.001
r_a^2	0.990±0.006	0.998±0.009	0.998±0.009	0.998±0.001
RMSE (cm^3)	0.214±0.006	0.088±0.021	0.087±0.021	0.088±0.022
D_{max} (cm^3)	0.501±0.013	0.194±0.050	0.194±0.050	0.195±0.050
e_α	0.042±0.015	0.073±0.030	0.053±0.021	0.095±0.047
e_β	0.040±0.018	0.046±0.019	0.048±0.022	0.047±0.020
$e_{Vobs(\alpha,\beta)}$	-	-	-	0.033±0.009
e_{u2}	0.046±0.007	0.052±0.023	0.051±0.013	0.082±0.025
e_{df}	0.071±0.011	0.072±0.019	0.070±0.021	0.073±0.020
e_{Df}	0.325±0.075	0.415±0.068	0.761±0.108	0.054±0.014
$e_{Vobs(u2,df,Df)}$	-	-	-	0.032±0.008

Means ± standard deviation of parameters of the Ehrlich tumor and criteria for model assessment obtained for different formulations of Gompertz equations.

https://doi.org/10.1371/journal.pone.0224978.t001

differentiate n_0 and n_{00} to compare GE_2 and GE_5 in order to avoid confusion in the interpretation of these two parameters. GE_5 revealed that n_∞ depends only on α and β and not on n_{00} ($n(t) = n_\infty = e^{\alpha/\beta}$ for $t \to \infty$).

Inclusion of n_{obs} in GE

Eq (3) was rewritten as

$$\begin{cases} \dfrac{dn}{dt} = \alpha n\left(1 - \dfrac{\beta}{\alpha}\ln\dfrac{n}{n_{obs}}\right), \\ n(t=0) = n_{000} \end{cases} \tag{7}$$

where n_{000} was the number of tumor cells that the researcher selected at $t = t_0$. The analytical solution of Eq (7) was given by

$$n(t) = \left[n_{obs}\left(\frac{n_{000}}{n_{obs}}\right)^{e^{-\beta t}}\right] e^{\left(\frac{\alpha}{\beta}\right)(1-e^{-\beta t})}. \tag{8}$$

Eq (8), named GE_8, agreed with GE_5 at $t = 0$ (for all n_{obs}) and when $n_{obs} = 1$ (for all t). The GE_8 coincided with the GE_2 at $t = 0$ (for all n_{obs}) and when $n_0 = n_{obs}(n_{000}/n_{obs})^{e^{-\beta t}}$. The parameter n_{obs} ($n_{obs} < n_{med} \leq n_{000}$) was the starting point of TGK. In general, n_{000} did not coincide with n_0 (GE_2) or n_{00} (GE_5). Therefore, it was convenient to differentiate the parameters n_0, n_{00} and n_{000}. In addition, the GE_8 evidenced that n_∞ depends on n_{obs}, α and β, but not on n_{000} ($n(t) = n_\infty = n_{obs}\, e^{\alpha/\beta}$ for $t \to \infty$). The parameters α and β in terms of u_2, U_1, θ, d_f, D_f and n_{obs} were given by

$$\begin{cases} \alpha = u_2\left[\ln\dfrac{U_1}{u_2}\right] - \beta\ln(n_{obs}) = u_2\ln\left(\dfrac{\frac{2}{3}d_f - 1}{d_f - 1}\right) - \beta\ln(n_{obs}) \\ \beta = u_2(1-\theta) = u_2\left(1 - \dfrac{d_f}{D_f}\right) \end{cases}. \tag{9}$$

Eq (9) resulted from assuming that the value of n in the steady state was $n_{ss} = n_{obs}\, e^{\alpha/\beta} = (u_2/U_1)^{1/(\theta-1)}$ and Eqs (7) and (8) were taken into account.

Simulations

Simulation of Eq (9). Eq (9) coincided with Eq (6) for $n_{obs} = 1$. The simulation of α (in $days^{-1}$) versus d_f was shown for $D_f = 5$ and four values for u_2 (1, 10, 50 and 100 $days^{-1}$) and n_{obs} (1, 5, 10 and 20 cells). For this, values of d_f were varied from 0 to 5 with a step of 0.5, taking into account that $d_f < D_f$. The simulation of β (in $days^{-1}$) against d_f/D_f was shown for four values of u_2 (1, 10, 50 and 100 $days^{-1}$) and the values of d_f/D_f were ranged from 0 to 5 with a step of 0.5.

Simulations of GE_2, GE_5 and GE_8. GE_5 was used as reference because GE_5 and GE_8 were reported for the first time in the literature. The simulations of GE_2, GE_5 and GE_8 were shown in a graph of n(t). Simulation of GE_2 was made for different values of n_0 ($1x10^3$, $1x10^4$, $1x10^5$ and $1x10^6$ cells). Additionally, GE_8 was simulated for three different situations: 1) $n_{obs} = 1$ cell (GE_8 and GE_5 coincided) and different values of n_{00} (5, 10, 15, 20 and 25 cells); 2) $n_{obs} = 1x10^4$ cells and different values of n_{000} ($1x10^4$, $5x10^4$, $1x10^5$ and $2x10^5$ cells); and 3) $n_{000} = 1x10^5$ cells

and different values of n_{obs} ($5x10^3$, $1x10^4$, $5x10^4$ and $1x10^5$ cells). In all these simulations, α = 1.0 $days^{-1}$ and β = 0.3 $days^{-1}$.

Experimental groups

In this study, V(t) was used by three reasons: 1) V(t) is related to n(t) and can be used interchangeably; 2) V(t) is less cumbersome to estimate than n(t) and it is frequently used in preclinical [9–11] and clinical [10] studies; and 3) the graphs of V(t) and n(t) shown sigmoidal shapes. Consequently, n(t) in GE_1, GE_2, GE_5 and GE_8 was replaced by V(t); n_0 in GE_2 by V_0; n_{00} in GE_5 by V_{00}; n_{000} and n_{obs} in GE_8 by V_{000} and V_{obs}, respectively. In addition, n_{med} was replaced by V_{med} and n_∞ by V_∞. The parameter V_∞ was the tumor volume when $t \rightarrow \infty$.

Two experimental groups were formed, each consisting of 10 male BALB/c/Cenp mice. The first group corresponded to the Ehrlich tumor, denominated G1, while the second group to the fibrosarcoma Sa-37 tumor, denominated G2. Experimental data of V(t) for Ehrlich and fibrosarcoma Sa-37 tumors were reported in [9], corresponding to their control groups.

Interpolation of experimental data

The Hermite interpolation method [13] was used to interpolate volume data of each individual tumor, in G1 and G2.

Estimation of values of α, β, d_f, D_f and u_2 from experimental data

Values of α and β (GE_1, GE_2, GE_5 and GE_8) and V_{obs} (GE_8) were obtained from the individual fitting of each tumor volume (Ehrlich and fibrosarcoma Sa-37). The value of V_{obs} estimated directly with GE_8 was named $V_{obs(\alpha,\beta)}$. The value $V_0 = V_{00} = V_{000} = 0.5$ cm^3 was the tumor volume chosen to describe TGK. This volume value was reached 15 days after $2x10^6$ cells for the Ehrlich tumor and $5x10^5$ cells for the fibrosarcoma tumor Sa-37 were inoculated in the BALB/c/Cenp mouse (see details in [9]).

Three equations in terms of d_f, D_f and u_2 resulted when Eq (6) was substituted in GE_1, GE_2 and GE_5. The values of these three parameters were determined when each of these equations was used to fit experimental data. Besides, Eq (12) was substituted in GE_8 and resulted an equation in terms of d_f, D_f, u_2 and V_{obs}, from which their values were estimated from fitting experimental data. Once known the values of d_f, D_f, u_2 and V_{obs}, they were substituted in their respective Eqs (6) and (9) to calculate their corresponding values of α and β. Values of α, β and V_{obs} obtained by this way were denominated α_c, β_c and $V_{obs(u2,df,Df)}$, respectively, to distinguish these values from those that were directly obtained from fitting of the experimental data with GE_1, GE_2, GE_5 and GE_8.

The estimation errors for α, β, d_f, D_f, u_2, V_{obs} and $V_{obs(u2,df,Df)}$ were denominated e_α, e_β, e_{df}, e_{Df}, e_{u2}, e_{Vobs} and $e_{Vobs(u2,df,Df)}$, respectively. The estimation error for each parameter was reported for each individual tumor of Ehrlich and fibrosarcoma Sa-37.

The difference between α and α_c, named $\Delta\alpha$ ($\Delta\alpha = \alpha - \alpha_c$), was calculated for each equation (GE_1, GE_2, GE_5 and GE_8) and experimental group (G1 and G2). In addition, it were computed differences between β and β_c, denominated $\Delta\beta$ ($\Delta\beta = \beta - \beta_c$), and $V_{obs(u_2,d_f,D_f)}$ and $V_{obs(\alpha,\beta)}$, denominated ΔV_{obs} ($\Delta V_{obs} = V_{obs(\alpha,\beta)} - V_{obs(u_2,d_f,D_f)}$).

Criteria for model assessment

Five quality-of-fit criteria were used for fitting of experimental data with GE_1, GE_2, GE_5 and GE_8: the sum of squares of errors, SSE (Eq (10)); standard error of the estimate, SE (Eq (11)); adjusted goodness-of-fit coefficient of multiple determination, r_a^2 (Eq (12)), that depended on

goodness-of-fit coefficient r^2 (Eq (14)); predicted residual error sum of squares, PRESS (Eq (14)); and multiple predicted residual sum error of squares, MPRESS (Eq (15)) [1, 3, 14], given by

$$SSE = \sum_{j=1}^{n_1} (\hat{V}_j^* - V_j^*)^2, \tag{10}$$

$$SE = \sqrt{\frac{\sum_{j=1}^{n_1} \left(\hat{V}_j^* - V_j^*\right)^2}{n_1 - k}}, \tag{11}$$

$$r_a^2 = 1 - \frac{n_1 - 1}{n_1 - k}(1 - r^2) = \frac{(n_1 - 1)r^2 - k + 1}{n_1 - k}, \tag{12}$$

$$1 - r^2 = \frac{\sum_{j=1}^{n_1} (\hat{V}_j^* - V_j^*)^2}{\sum_{j=1}^{n_1} (V_j^*)^2 - \frac{1}{n_1}\left(\sum_{j=1}^{n_1} V_j^*\right)^2}, \tag{13}$$

$$PRESS = \frac{\sum_{j=1}^{n_1-1} \left[(\hat{V}_j^*)^{\acute{a}} - V_j^*\right]^2}{n_1 - k}, \tag{14}$$

$$MPRESS(m) = \frac{\sum_{j=m+1}^{n_1} \left[(\hat{V}_j^*)^{\acute{a}} - V_j^*\right]^2}{n_1 - m}, \tag{15}$$

where V_j^* was the j-th measured tumor volume at discrete time t_j, j = 1, 2, . . ., n_1; $\hat{V}_j^*$ was the j-th estimated tumor volume by GE_1, GE_2, GE_5 and GE_8; n_1 the number of experimental points (n_1 = 10) and k the number of parameters (k = 2 for GE_1, GE_2 and GE_5, and k = 3 for GE_8). The fitting was considered to be satisfactory when $r_a^2 > 0.98$. Higher r_a^2 meant a better fit. $(V_j^*)^{\acute{a}}$ was the estimated value of V_j^* when $GE_1/GE_2/GE_5/GE_8$ was obtained without the j-th observation. MPRESS removed the last n_1–m measurements. Each equation (GE_1, GE_2, GE_5 and GE_8) was fitted to the first m measured experimental points (m = 3, 4 or 5) and then from calculated model parameters the error between tumor volume estimated and measured values in the remaining n_1–m points was calculated. Least Sum of Squares of Errors was obtained when SSE was minimized in the Marquardt-Levenberg optimization algorithm.

The Root Means Square Error, RMSE (Eq (16)) and the maximum distance, D_{max} (Eq (17)) were also calculated following the methodology suggested in [1, 3, 14], given by

$$RMSE = \sqrt{\sum_{i=1}^{M} \frac{(F_i - G_i)^2}{M}}, \tag{16}$$

$$D_{máx} = \text{máx}|F_i - G_i|, \tag{17}$$

where M was the number of interpolated data of tumor kinetics (graph of V(t)). F_i was the *i-th*

tumor volume of the experimental data, which was chosen as reference. G_i was the *i-th* tumor volume calculated with GE_1, GE_2, GE_5 and GE_8.

Each fit with the $GE_1/GE_2/GE_5/GE_8$ was performed for each animal growth curve. A computer program was implemented in the Matlab® software (version R2012b 64-bit, Institute for Research in Mathematics and Applications, University of Zaragoza, Spain) to calculate the tumor volume. In addition, the mean ± standard error of each parameter of the equation (α, β, $V_{obs(\alpha,\beta)}$, u_2, d_f, D_f, $V_{obs(u2,df,Df)}$, α_c, β_c), fit criterion (SE, PRESS, MPRESS, r_a^2, RMSE and D_{max}) and estimation error (e_α, e_β, e_{df}, e_{Df}, e_{u2}, e_{Vobs} and $e_{Vobs(u2,df,Df)}$) were calculated from their individual values, in each experimental group, following the methodology reported in [1, 3]. These calculations were performed on a PC with an Intel(R) core processor (TM) i7-3770 at 3.40 GHz with a Windows 10 operating system. All calculations took approximately 10 min, for each equation.

Results

Simulation of Eq (6)

Fig 1 showed the simulations of β versus d_f/D_f (Fig 1*A*) and α versus d_f (Fig 1*B*) for different values of u_2. The positive values of α (in the interval $0 \leq d_f < 1$) and β (in the interval $d_f/D_f < 1$) increased non-linearly with the increase of d_f and decreased linearly with the increase of d_f/D_f, respectively. The negative values of α increased non-linearly with the increase in d_f ($d_f > 1.5$). The negative values of β decreased linearly with the increase of d_f/D_f ($d_f/D_f > 1$). These behaviors were noticeable for the greater value of u_2. Additionally, the parameter α had a discontinuity in the interval $1 < d_f < 1.5$ and $\beta = 0$ when $d_f/D_f = 1$ for all values of u_2.

Simulation of Eq (9)

Results of the simulation of β versus d_f/D_f in Eq (11) coincided with that shown in Fig 1*A* (see Eqs (6) and (9)). The simulation of α versus d_f for $n_{obs} = 1$ (Fig 2*A*) reproduced the same result as in Fig 1*B*. However, values of α were more negative, in the interval $0 \leq d_f < 1$, when n_{obs} increased, being noticeable for the higher value of u_2 (Fig 2*B*, 2*C* and 2*D*). In Fig 2*A*, 2*B*, 2*C* and 2*D*, as in Fig 1*B*, it was observed a discontinuity of α in the interval $1 < d_f < 1.5$.

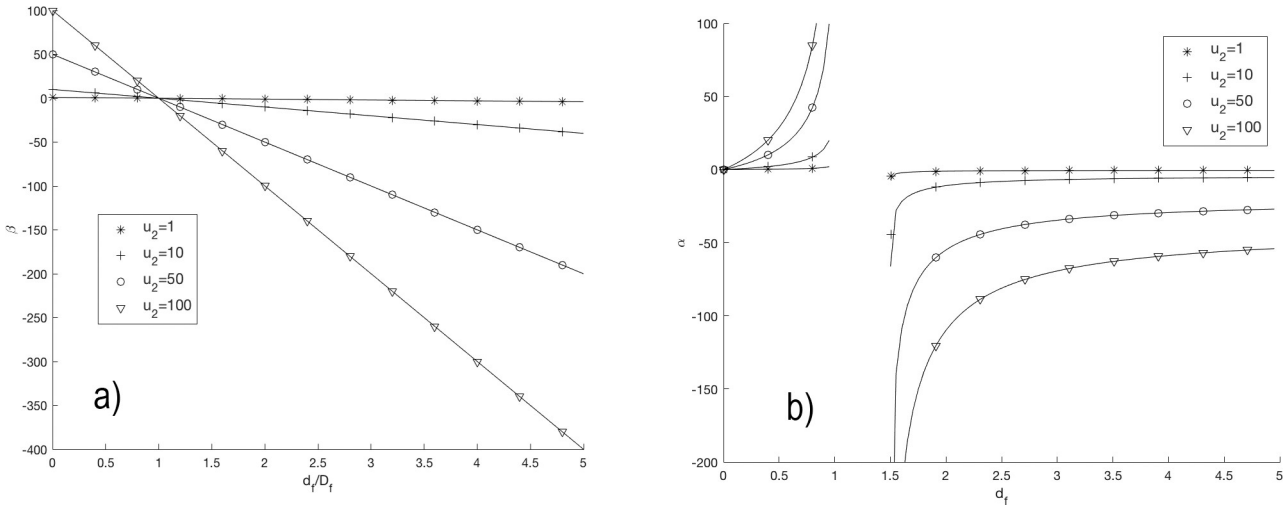

Fig 1. Simulation of Eq (6). For different values of u_2 (1, 10, 50 and 100 $days^{-1}$) it is plotted (*A*) Graph of α (in $days^{-1}$) versus d_f and (*B*) Graph of β (in $days^{-1}$) versus d_f/D_f.

https://doi.org/10.1371/journal.pone.0224978.g001

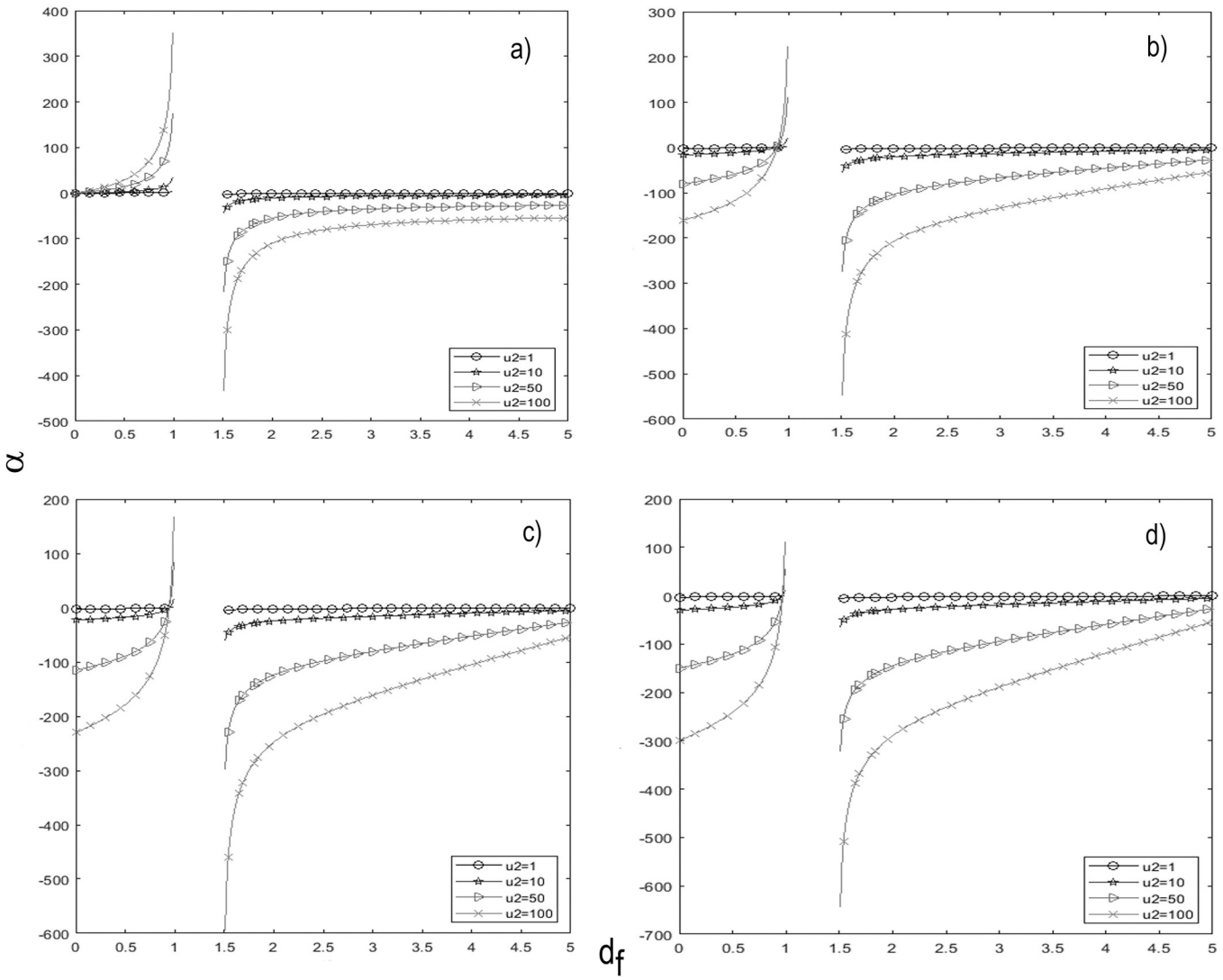

Fig 2. Simulation of Eq (9). For different values of u_2 (1, 10, 50 and 100 days^{-1}) it is plotted the graph of α (in days^{-1}) versus d_f for (*A*) n_{obs} = 1 cell. (*B*) n_{obs} = 5 cells. (*C*) n_{obs} = 10 cells. (*D*) n_{obs} = 20 cells.

https://doi.org/10.1371/journal.pone.0224978.g002

Simulations of GE_2, GE_5 and GE_8

Fig 3 showed the behavior of n(t) when GE_2 (Fig 3*A*, GE_5 (Fig 3*B*) and GE_8 (Fig 3*C* and 3*D*) were used. Fig 3*A* revealed that the highest value of n_∞ and the fastest TGK occurred for the highest values of n_0 and α. Fig 3*B* showed that TGK was faster with the increase of n_{00} and all TGK tended to the same value of n_∞ for all value of n_{00}, keeping constant values of α and β. In this case, TGK was faster when the value of n_{00} increased with respect to n_{obs} (Fig 3*B*), being noticeable when n_{obs} increased with respect to 1 (Fig 3*C*). It is important to note that $n_0 = n_{00}$ (Fig 3*B*) and $n_0 = n_{000}$ (Fig 3*C* and 3*D*).

The results of Fig 3*D* showed that TGK grows slower (when $n < n_{000}$) and then faster (when $n > n_{000}$) for the greater value of n_{obs}; all TGK were cut at t = 0 (same value of n_{000}), for all value of n_{obs}; and the value of n_∞ depended on n_{obs} and not n_{000} for each TGK. The results shown in Fig 3 were noticeable when the value of α increased with respect to that of β (results not shown).

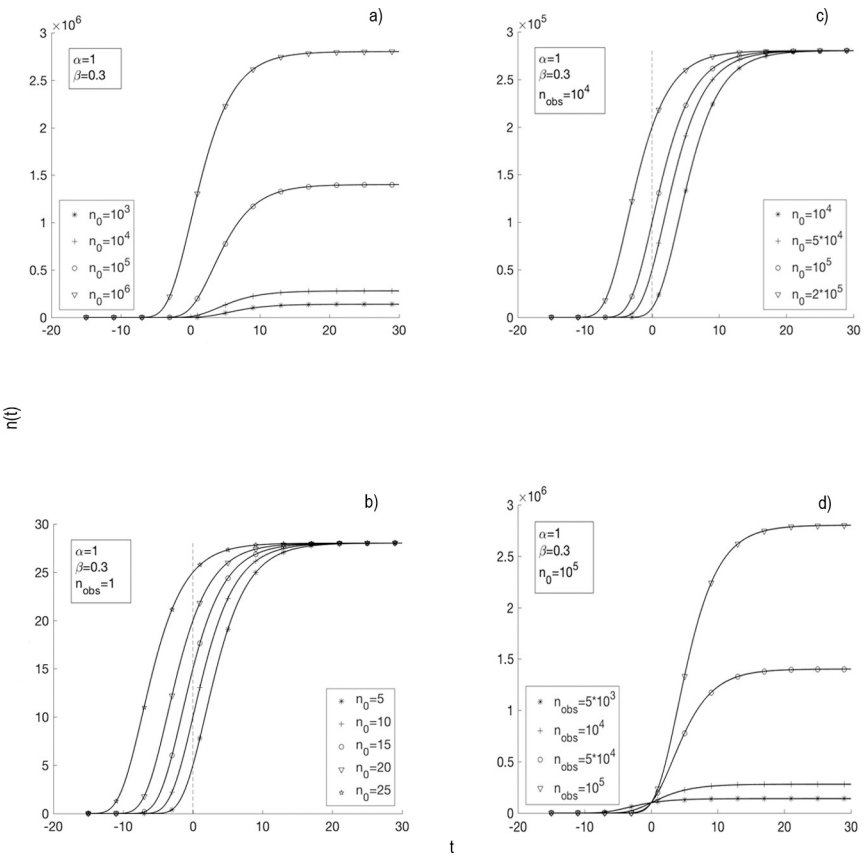

Fig 3. Evolution of the number of cells with time. Simulation of the number of cells at time t, in days, (n (t)) for α = 1.0 days^{-1} and β = 0.3 days^{-1}. (*A*) Simulation of GE_2 for different values of n_0 ($1x10^3$, $1x10^4$, $1x10^5$ and $1x10^6$ cells). (*B*) Simulation of GE_8 for n_{obs} = 1 cell (coincides with GE_5) and different values of $n_{00} = n_0$ (5, 10, 15, 20 and 25 cells). (*C*) Simulation of GE_8 for $n_{obs} = 1x10^4$ cells and different values of $n_{000} = n_0$ ($1x10^4$, $5x10^4$, $1x10^5$ and $2x10^5$ cells). (*D*) Simulation of GE_8 for $n_{000} = n_0 = 1x10^5$ cells and different values of n_{obs} ($5x10^3$, $1x10^4$, $5x10^4$ and $1x10^5$ cells).

https://doi.org/10.1371/journal.pone.0224978.g003

Fitting of experimental data with GE_1, GE_2, GE_5 and GE_8 and estimation of values of α, β, d_f, D_f and u_2

The mean ± standard deviation of each parameter of the equation, fit criterion and estimation error were shown in Tables 1 and 2 of each equation (GE_1, GE_2, GE_5 and GE_8) used to fit experimental data of the Ehrlich and fibrosarcoma Sa-37 tumors, respectively. Tables 1 and 2 shown for these two tumor histological varieties: $0 < d_f < 1$; $1 < D_f < 2$; $0 < u_2 < 1$; the highest values of α, u_2 and the lowest values of d_f and D_f for GE_8; the lowest SE values for GE_5 and GE_8; the lowest values of PRESS, MPRESS, RMSE and D_{max}; the highest values of r^2 and r_a^2 for GE_2, GE_5 and GE_8; and values of the parameter α differed when GE_1, GE_2, GE_5 and GE_8 were used. Nevertheless, the parameter β was the same when GE_2, GE_5 and GE_8 were used, but not for GE_1.

For the Ehrlich tumor, Δα = 0.003, 0.005, 0.001 and 0.005 days^{-1} for GE_1, GE_2, GE_5 and GE_8, respectively. The variable Δβ = 0.012, 0.026, 0.014 and 0.000 days^{-1} for these respective equations and ΔV_{obs} = 0.007 cm^3. For the tumor fibrosarcoma Sa-37, Δα = 0.009, 0.003, 0.006 and 0.019 days^{-1} for GE_1, GE_2, GE_5 and GE_8, respectively. The variable Δβ = 0.025, 0.038, 0.028 and 0.000 days^{-1} for these respective equations and ΔV_{obs} = 0.006 cm^3.

Table 2. Parameters of the models for the fibrosarcoma Sa-37 tumor.

Parameters	Different formulations of Gompertz equations			
	GE_1	GE_2	GE_5	GE_8
α ($days^{-1}$)	0.188±0.016	0.491±0.034	0.316±0.018	0.833±0.132
β ($days^{-1}$)	0.127±0.017	0.252±0.018	0.252±0.018	0.252±0.018
$V_{obs(\alpha,\beta)}$ (cm^3)	-	-	-	0.148±0.088
u_2 ($days^{-1}$)	0.274±0.093	0.530±0.152	0.471±0.132	0.576±0.070
d_f	0.759±0.074	0.822±0.070	0.746±0.058	0.688±0.042
D_f	1.704±0.672	1.810±0.612	1.837±0.613	1.256±0.191
$V_{obs(u_2, d_f, D_f)}$ (cm^3)	-	-	-	0.142±0.029
α_c ($days^{-1}$)	0.197±0.020	0.494±0.029	0.322±0.011	0.814±0.082
β_c ($days^{-1}$)	0.152±0.018	0.290±0.020	0.280±0.017	0.252±0.018
SE	0.162±0.008	0.082±0.038	0.083±0.038	0.083±0.038
PRESS	0.761±0.227	0.063±0.059	0.063±0.059	0.064±0.060
MPRESS	0.623±0.203	0.063±0.059	0.064±0.059	0.064±0.060
r^2	0.995±0.004	0.998±0.001	0.998±0.001	0.999±0.001
r_a^2	0.996±0.004	0.998±0.001	0.998±0.001	0.999±0.001
RMSE (cm^3)	0.161±0.008	0.082±0.038	0.082±0.038	0.082±0.038
D_{max} (cm^3)	0.499±0.013	0.206±0.109	0.206±0.100	0.207±0.110
e_α	0.025±0.011	0.046±0.022	0.061±0.012	0.079±0.035
e_β	0.034±0.009	0.053±0.013	0.057±0.029	0.055±0.023
$e_{Vobs(\alpha,\beta)}$	-	-	-	0.027±0.007
e_{u2}	0.031±0.003	0.035±0.013	0.039±0.010	0.061±0.015
e_{df}	0.065±0.012	0.069±0.014	0.067±0.016	0.071±0.025
e_{Df}	0.235±0.086	0.336±0.045	0.679±0.119	0.125±0.031
$e_{Vobs(u2,df,Df)}$	-	-	-	0.041±0.017

Means ± standard deviation of parameters of the fibrosarcoma Sa-37 tumor and criteria for model assessment obtained for different formulations of Gompertz equations.

https://doi.org/10.1371/journal.pone.0224978.t002

Discussion

This study shows that GE_2, GE_5 and GE_8 can be used interchangeably to describe experimental data of Ehrlich and fibrosarcoma Sa-37 tumors, taking into account their higher values of r^2 and r_a^2, and lower values of each parameter of the equation, fit criterion, estimation error, $\Delta\alpha$, $\Delta\beta$ and ΔV_{obs} (ΔV_{obs} is only calculated for GE_8).

The theoretical and experimental results of this work confirm different findings reported previously in the literature, such as: 1) the fractal origin of GE_1, GE_2, GE_5 and GE_8, as reported in [4, 15]; 2) the fractal property of tumors once reached n_{med}/V_{med}, a matter that agrees with [16, 17]; 3) the role of the fractal dimension for the understanding of TGK, as suggested by Sokolov [18] and Breki et al. [19]; and 4) $1 < D_f < 2$, in agreement with [4, 20, 21] and the preferential growth along the largest diameter of the tumor, despite its ellipsoidal geometry [1, 3, 9, 11]. This fourth finding is in contradiction with $2 < D_f < 3$ reported by Breki et al. [19] in patients with metastatic melanoma; 5) The condition $0 < u_2 < 1$ for both types of tumors is consistent with the Steel equation [12]. If $u_2 = 0$, then the tumor growth fraction must be high so that its mean doubling time (TD) is short, in contrast to [10, 12]. If $u_2 = 1\ day^{-1}$ (all cancer cells are in apoptosis), $TD \rightarrow \infty$ and $\alpha = 0$ (tumor self-destruction), in contrast to the failure of the apoptosis mechanism in malignant tumors (because of the gene p-53 is repressed) and the existence of other cell loss mechanisms (metastasis, necrosis and exfoliation) [10, 11, 22].

The increase in u_2 brings about a decrease in TD and therefore a higher value of α (Figs 1*B*, 2*A*, 2*B*, 2*C* and 2*D*).

Other novel findings have been revealed in this investigation that may be of interest for understanding of TGK, such as: 1) TGK sigmoidal form and n_∞/V_∞ do not depend on n_0 and if on α, β and n_{obs}/V_{obs}, when a given tumor histological variety grows in a certain type of syngeneic host to it. In this way, the action form of parameter n_0/V_0 (form or location) is eliminated in GE_2, as reported in [2]. 2) The GE_8 states that n_0 in the GE_2 is not a constant parameter but depends non-linearly with n_{obs}/V_{obs}, n_{000}/n_{obs} (V_{000}/V_{obs}), β and t. 3) The growth of a malignant tumor occurs for $0 < d_f < 1$ and not when $d_f = 0$ (α = 0: the tumor does not form), $1 < d_f < 1.5$ (discontinuity of α due to forbidden conformations or very unlikely tumor) and $d_f > 1.5$ (α < 0: the tumor self-destructs), in contrast to the values of d_f ($1 < d_f < 2$) reported in [4, 14, 23]. The forbidden conformations of the tumor can be explained by its stereochemistry due to the steric collides between all its elements and the tumor-host interaction. 4) The increase of α with the increase of d_f, at $0 < d_f < 1$, confirms that the growth efficiency of a malignant tumor increases with its d_f, in agreement with [17, 24]. 5) Eq (11) states that this increase of α with d_f occurs if n_{obs} satisfies strictly the condition $n_{obs} < [(2/3d_f - 1)/(d_f - 1)]^{u_2/\beta}$; otherwise, α < 0 for all β positive (Fig 2B, 2*C* and 2*D*). The case α < 0 means that the tumor self-destructs, in contrast to the experiment.

The established condition for n_{obs} suggests that: 1) n_{obs}/V_{obs} depends on d_f and the ratio u_2/β; 2) the fractal property of a malignant tumor also happens before or long before its detection (n_{med}/V_{med}), as reported in [1, 25]; 3) the ratio u_2/β may be an indirect indicator of the apoptosis-angiogenesis relationship reported in [26, 27]; 4) endogenous anti-angiogenic factors or inhibitors of angiogenesis (endostatin, angiostatin, among others) are present in the tumor before or long before reaching n_{med}/V_{med}; 5) the term $e^{-\beta t}$ (see GE_8 and the established condition for n_{obs}) and the decrease of the parameter β with the increase of d_f/D_f corroborate the essential role of angiogenesis process and the displacement of the balance between endogenous anti-angiogenic factors and endogenous pro-angiogenic factors towards these latter, when the tumor volume grows at time t, consistent with [10, 17, 22, 28, 29].

From the mathematical point of view, the condition $0 < d_f < 1$ may suggest that the contours of Ehrlich and fibrosarcoma Sa-37 malignant tumors have zero area and/or they are totally disconnected. The first assumption confirms that these two types of tumors can be delimited from their surrounding healthy tissue, as in [9, 11]. The second hypothesis is based on proposition 2.5 [30]: "A set $F \subset \Re^n$ with $\dim_H F<1$ is totally disconnected". In this proposition, F is any set and $\dim_H$ is the fractal dimension Hausdorff. It is important to note that, although the tumor boundary is wide, $d_f < 1$ if its only fractality is given by a totally disconnected line contained in that wide band.

From the biophysical point of view, the tumor contour totally disconnected can indicate the existence in it of pores/channels formed randomly of different sizes and shapes, changing in the time. This porous contour of a tumor may be related to the angiogenesis process (neoformation of blood vessels), the formation of spicules by fragmentation of the contour into simple forms of molds (for example, triangles), roundness, irregular edge, anisotropy, roughness and compactness, findings reported in [1, 3, 10, 22, 31–34]. We believe that the tumor angiogenesis process can be regulated by the amount of pores/channels existing in its contour to interconnect with the surrounding healthy tissue. This hypothesis can corroborate that the angiogenesis of a malignant tumor is an emergency and regulated by the structural and conformational dynamic transformations that occur during TGK, as reported in [1]. On the contrary, if these pores/channels do not exist, the tumor would behave as an isolated system and would self-destruct, in contrast to the experiment.

Fig 3 deserves a careful interpretation, taking into account experimental results reported in the preclinical [1, 3, 9, 11, 14] and clinical [10] studies. The result of Fig 3*A* corresponds with the selection of different values of n_0/V_0 in the same TGK for different instants t_0. For this case, in the experiment is guaranteed fixed c_o, cell viability, the tumor histological variety and the type of syngeneic host to it. The higher value of n_0/V_0 in the same TGK means a larger tumor size, which is reached at a higher t_0.

Results of Fig 3*B* and 3*C* are associated to the same tumor histological variety that grows in several types of syngeneic hosts to it. For this case, c_o and cell viability fixed are guaranteed, taking into account the role of the immune system in the delay of TGK, depending on its immunocompetence degree [10, 11, 22, 35]. As a result, tumors reach different values of n_{00}/V_{00} o n_{000}/V_{000} at the same time t_0. The higher value of n_{00}/V_{00} (n_0/V_0 in Fig 3*B*) or n_{000}/V_{000} (n_0/V_0 in Fig 3*C*) corresponds to the lower immunocompetence degree of the host (e.g., an immunosuppressed host).

Results of Fig 3*B* refer to two possible situations: 1) different tumor histological varieties that grow in the same type of syngeneic host to them. For this case, c_o is different so that each tumor histological variety reaches the same value of n_{000}/V_{000} at the same time t_0. 2) A given tumor histological variety that grows in different types of syngeneic hosts to it. For this case, c_o is the same for each tumor histological variety. For these two cases, n_{obs}/V_{obs} for each tumor histological variety is reached in a different t_{obs}, in accordance with the experiment [9, 11]. These two situations become noticeable when β approaches α (results not shown). Furthermore, this figure reveals that for the highest value of n_{obs}/V_{obs} (reached in a greater t_{obs}) TGK is slower for $n(t) < n_{000}$ ($V(t) < V_{000}$) and then faster for $n(t) > n_{000}$ ($V(t) > V_{000}$). By contrast, the tumor that has the lowest n_{obs}/V_{obs} is the fastest growing for $n(t) < n_{000}$ ($V(t) < V_{000}$) and then its TGK is slowest for $n(t) > n_{000}$ ($V(t) > V_{000}$).

The advantages of GE_8 over the various formulations of GE [2, 3], the Hahnfeldt model [36–38] and mKJMA equation [1], used to describe undisturbed TGK, are: 1) inclusion of two parameters (n_{obs}/V_{obs} y n_{000}/V_{000}) that are measured and estimated from experimental data. 2) TGK and n_∞/V_∞ can be known *a priori* if n_{obs}/V_{obs} (starting point of TGK), reached at t_{obs}, is estimated for each type of tumor that grows in a syngeneic host to it, as reported in [1, 3, 11].

The relation of the tumor growth with d_f and D_f is previously obtained by using a mesoscopic formalism and fractal dimension [39]. Besides, Izquierdo-Kurlich [39] report the differences between d_f and D_f and propose a relation between d_f and the dynamic quotient on the interface, named k_c, (see Eq (48)). This relationship differs from that reported in [4] (see Eq (3)), which is used to obtain Eq (8). If the relation published in [39] is taken into account in this study, Eq (8) is also obtained, except a small change in α numerator (1/2 instead of 1). As a result, 0.75 and 1 are the discontinuities of α, instead of 1 and 1.5, respectively. Nevertheless, these change do not affect significantly the results of this manuscript and confirm that tumors exits for $0 < d_f < 1$. It can be verified that d_f for Ehrlich and fibrosarcoma Sa-37 tumors are less than 0.75 and 1 when Eq (48) in [39] and Eq (3) in [4] are used.

In this study, the tumor growth in the time results of the complex interactions that happen in the tumor and between it and the surrounding healthy tissue, as in [3,14]. Nevertheless, in it does not explicitly discuss the interactions among the individuals neither the cooperative capacity of they in a population to explain its growth behavior, as in [25, 5–8]. These works confirm the fractal property of the tumors, as in this study. Therefore, an additional study may include these interactions for Eq (8).

Further studies can be carried out to validate GE_8 in TGK of different tumor histological varieties that grow in both immune-competent and immune-deficient organisms. This will allow us to know how D_f, d_f, u_2, $V_{obs(\alpha,\beta)}$ and $V_{obs(u2,df,Df)}$ change when using different types of tumors and degrees of immune-competence of several organisms, as well as confirming the

relationship of these five parameters with the aggressiveness [1], angiogenesis [17], coherence [15, 16], anisotropy, heterogeneity, hardness, changes in the mechanical-elastic-electrical properties of a tumor, among others findings [1].

Conclusions

GE_8 describes well the growth kinetics of the Ehrlich and fibrosarcoma Sa-37 tumors and includes two parameters that are directly estimated from the experiment that confirm the fractal property of the tumors and the fractal origin of different Gompertz formulations.

Appendix A

In [4] it is assumed that the growth ratio of the number $n(t)$ of tumor cells obeys to the differential equation

$$\frac{dn}{dt} = u_1 m - u_2 n,\ n(0) = n_0, \tag{A1}$$

where m represents the number of tumor cells at the boundary of the tumor, u_1 is the constant of the velocity of the mitosis and u_2 is the constant of the velocity of apoptosis.

Assuming that the boundary has a fractal structure with dimension d_f, then $m = k_1 r^{d_f}$, r being the average radius of the tumor. On the other side, n depends on the morphology of the tumor, described by the fractal dimension D_f, and $n = k_2 r^{D_f}$. The morphological constants k_1 and k_2 are related to the magnification of the image [4].

Substituting these values of m and n and eliminating r, Eq (1) can be written as a Bertalanffy-Richards equation.

$$\frac{dn}{dt} = U_1 n^{\theta} - u_2 n = n u_2 \left(\left(\frac{n_{ss}}{n} \right)^{1-\theta} - 1 \right),$$

where $n_{ss} = (u_2/U_1)^{1/(1-\theta)}$ is the value of n at the steady state, the dimensionless morphological parameter θ is defined by $\theta = d_f/D_f$ and U_1 is given by $U_1 = u_1 k_1 / k_2^{\theta}$.

Taking into account that

$$\ln x = \lim_{s\to\infty} s\left(x^{\frac{1}{s}} - 1 \right),$$

the above equation is approximated in [4] by the Gompertz equation

$$\begin{cases} \dfrac{d\ln(n)}{dt} = u_2(\theta - 1)\ln\left(\dfrac{n}{n_{ss}}\right) \\ \ln(n)_{t=0} = 0 \quad n(t=0) = 1 \end{cases}, \tag{A2}$$

This approximation is valid when $\theta \to 1$ or $n \to n_{ss}$.

In [36] it is justified that the quotient U_1/u_2 can be expressed as a function of d_f and in [4] it is shown that the solution of the differential system (2)

$$n(t) = e^{\frac{\ln(U_1/u_2)(1-e^{u_2(\theta-1)t})}{1-\theta}}$$

can be expressed as a Gompertz equation (Eq (1) in this paper)

$$n(t) = e^{\left(\frac{\alpha}{\beta}\right)(1-e^{-\beta t})}$$

with the intrinsic growth rate of the undisturbed tumor, named α (α > 0), and the deceleration

factor, named β (β > 0), related to the tumor fractal dimensions by

$$\begin{cases} \alpha = u_2\left[\ln\frac{U_1}{u_2}\right] = u_2\ln\left(\frac{1.5d_f - 1}{d_f - 1}\right) \\ \beta = u_2(1-\theta) = u_2\left(1 - \frac{d_f}{D_f}\right) \end{cases}. \quad \text{(A3)}$$

Supporting information

S1 Data. Supporting information.
(TXT)

Acknowledgments

We would like to give our special thanks to the Editor in Chief, Associate editor and reviewers of this article for their expert help and invaluable feedback.

Author Contributions

Conceptualization: Antonio Rafael Selva Castañeda, Erick Ramírez Torres, Narciso Antonio Villar Goris, Maraelys Morales González, Juan Bory Reyes, Victoriano Gustavo Sierra González, María Schonbek, Juan Ignacio Montijano, Luis Enrique Bergues Cabrales.

Formal analysis: Antonio Rafael Selva Castañeda, Erick Ramírez Torres, Narciso Antonio Villar Goris, Maraelys Morales González, Juan Bory Reyes, Victoriano Gustavo Sierra González, María Schonbek, Juan Ignacio Montijano, Luis Enrique Bergues Cabrales.

Funding acquisition: Juan Ignacio Montijano.

Investigation: Antonio Rafael Selva Castañeda, Erick Ramírez Torres, Narciso Antonio Villar Goris, Maraelys Morales González, Juan Bory Reyes, Victoriano Gustavo Sierra González, María Schonbek, Juan Ignacio Montijano, Luis Enrique Bergues Cabrales.

Methodology: Antonio Rafael Selva Castañeda, Erick Ramírez Torres, Narciso Antonio Villar Goris, Maraelys Morales González, Juan Bory Reyes, Victoriano Gustavo Sierra González, María Schonbek, Juan Ignacio Montijano, Luis Enrique Bergues Cabrales.

Software: Antonio Rafael Selva Castañeda, Juan Ignacio Montijano, Luis Enrique Bergues Cabrales.

Supervision: Juan Ignacio Montijano, Luis Enrique Bergues Cabrales.

Writing – original draft: Antonio Rafael Selva Castañeda, Erick Ramírez Torres, Narciso Antonio Villar Goris, Maraelys Morales González, Juan Bory Reyes, Victoriano Gustavo Sierra González, María Schonbek, Juan Ignacio Montijano, Luis Enrique Bergues Cabrales.

Writing – review & editing: Antonio Rafael Selva Castañeda, Erick Ramírez Torres, Narciso Antonio Villar Goris, Maraelys Morales González, Juan Bory Reyes, Victoriano Gustavo Sierra González, María Schonbek, Juan Ignacio Montijano, Luis Enrique Bergues Cabrales.

References

1. González MM, Joa JA, Cabrales LE, Pupo AE, Schneider B, Kondakci S et al., Is cancer a pure growth curve or does it follow a kinetics of dynamical structural transformation? BMC Cancer 2017; 17:174. https://doi.org/10.1186/s12885-017-3159-y PMID: 28270135

2. Tjørve KMC, Tjørve E, The use of Gompertz models in growth analyses, and new Gompertz-model approach: An addition to the Unified-Richards family. Plos One 2017; 12:6.
3. Cabrales LE, Nava JJ, Aguilera AR, Joa JA, Ciria HM, González MM et al., Modified Gompertz equation for electrotherapy murine tumor growth kinetics: Predictions and new hypotheses. BMC Cancer 2010; 10:589. https://doi.org/10.1186/1471-2407-10-589 PMID: 21029411
4. Izquierdo-Kulich E, Regalado O, Nieto-Villar JM, Fractal origin of the Gompertz equation. Rev Cub Fis 2013; 30:26.
5. Mombach JCM, Lemke N, Bodmann BEJ, Idiart MAP, A mean-field theory of cellular growth. Europhys Lett 2002; 59:923–928.
6. d'Onofrio A, Fractal growth of tumors and other cellular populations: linking the mechanistic to the phenomenological modeling and vice versa. Chaos, Solitons & Fractals 2009; 41:875–880.
7. Ribeiro FL, A Non-phenomenological Model of Competition and Cooperation to Explain Population Growth Behaviors. Bull Math Biol 2015; 77:409–433. https://doi.org/10.1007/s11538-014-0059-z PMID: 25724311
8. Ribeiro FL, An attempt to unify some population growth models from first principles. Rev Bras Ensino Fis 2017; 39:e1311.
9. Ciria HMC, Quevedo MS, Cabrales LB, Bruzón RP, Salas ME, Pena OG et al., Antitumor effectiveness of different amounts of electrical charge in Ehrlich and fibrosarcoma Sa-37 tumors. BMC Cancer 2004; 4:87. https://doi.org/10.1186/1471-2407-4-87 PMID: 15566572
10. Cotran RS, Kumar V, Collins T, Patología Estructural y Funcional. Sexta Edición McGraw-Hill- Interamericana de España (S.A.U. Madrid); 1999. pp 277–347.
11. Cabrales LEB, The electrotherapy a new alternative for the treatment of the malignant tumors. Preclinical study. PhD thesis. Havana University, Biology Department, 2003.
12. Steel GG, Basic Clinical Radiobiology. Second Edition (Oxford University Press, Inc. New York); 1997. pp 1–30.
13. Yang WY, Cao W, Chung TS, Morris J, Applied Numerical Methods using MATLAB®. Wiley-Interscience (John Wiley & Sons, New Jersey); 2005. pp 117–156.
14. Cabrales LEB, Aguilera AR, Jiménez RP, Jarque MV, Ciria HMC, Reyes JB et al., Mathematical modeling of tumor growth in mice following low-level direct electric current. Math Simul Comp 2008; 78:112–120.
15. Waliszewski P, Konarski J, The Gompertzian curve reveals fractal properties of tumor growth. Chaos, Solitons and Fractals 2003; 16:665–674.
16. Molski M, Biological growth in the fractal space-time with temporal fractal dimension. Chaotic Model Simul 2012; 1:169–175.
17. Shim EB, Kim YS, Deisboeck TS, Analyzing the dynamic relationship between tumor growth and angiogenesis in a two dimensional finite element model; 2007. Preprint. Available from: arXiv:q-bio/0703015v1 (q-bio.TO). Preprint, posted February 10, 2016.
18. Sokolov I, Fractals: a possible new path to diagnose and cure cancer? Future Oncology 2015; 11: 3049–3051. https://doi.org/10.2217/fon.15.211 PMID: 26466999
19. Breki CM, Dimitrakopoulou-Starauss A, Hassel J, Theoharis T, Sachpekidis C, Pan L et al., Fractal and multifractal analysis of PET/CT images of metastatic melanoma before and after treatment with ipilimumab. EJNMMI Research 2016; 6:61. https://doi.org/10.1186/s13550-016-0216-5 PMID: 27473846
20. Tavakol ME, Lucas C, Sadri S, NG EYK, Analysis of breast thermography using fractal dimension to establish possible difference between malignant and benign patterns. J Healthc Eng 2010; 1: 27–43.
21. Baish JW, Jain RK, Fractals and cancer. Cancer Research 2000; 60:3683–3688. PMID: 10919633
22. Hanahan D, Weinberg RA, Hallmarks of Cancer: The Next Generation. Cell 2011; 144:646–674. https://doi.org/10.1016/j.cell.2011.02.013 PMID: 21376230
23. Stępień R, Stępień P, Analysis of contours of tumor masses in mammograms by Higuchi's fractal dimension. Biocybern Biomed Eng 2010; 30:49–56.
24. Gazit Y, Berk DA, Leunig M, Baxter LT, Jain RK, Scale-invariant behavior and vascular network formation in normal and tumor tissue. Phys Rev Lett 1995; 75:2428–2431. https://doi.org/10.1103/PhysRevLett.75.2428 PMID: 10059301
25. Ribeiro FL, dos Santos RV, Mata AS, Fractal dimension and universality in avascular tumor growth; 2016. Phys Rev E 2017; 95:1–9.
26. Zhong JT, Yu J, Wang HJ, Shi Y, Zhao TS, He BX et al., Effects of endoplasmic reticulum stress on the autophagy, apoptosis, and chemotherapy resistance of human breast cancer cells by regulating the PI3K/AKT/mTOR signaling pathway. Tumor Biol 2017; 39:1010428317697562.

27. Win TT, Jaafar H, Yusuf Y, Relationship of angiogenic and apoptotic activities in soft-tissue sarcoma. South Asian J Cancer 2014; 3:171–174. https://doi.org/10.4103/2278-330X.136799 PMID: 25136525

28. Huang D, Lan H, Liu F, Wang S, Chen X, Jin K, et al., Anti-angiogenesis or pro-angiogenesis for cancer treatment: focus on drug distribution. Int J Clin Exp Med 2015; 8:8369–8376. PMID: 26309490

29. Nyberg P, Xie L, Kalluri R., Endogenous inhibitors of angiogenesis. Cancer Res 2005; 65:3967–3979. https://doi.org/10.1158/0008-5472.CAN-04-2427 PMID: 15899784

30. Falconer K, Fractal geometry. Mathematical foundations and applications. Chapter 2, Second edition (John Wiley & Sons, Ltd., Chichester, England); 2003. pp 33.

31. Kremheller J, Vuong AT, Yoshihara L, Wall WA, Schrefler BA, A monolithic multiphase porous medium framework for (A-) vascular tumor growth. Comput Methods Appl Mech Eng 2018; 340:657–683.

32. Verma A, Pitchumani R, Fractal description of microstructures and properties of dynamically evolving porous media. Int J Heat Mass Transf 2017; 81:51–55.

33. Grizzi F, Fractal geometry as a tool for investigating benign and malignant breast mammography lesions. Fractal Geometry and Nonlinear Anal in Med and Biol 2015; 1:16–18.

34. Rangayyan RM, Nguyen TM, Fractal analysis of contours of breast masses in mammograms. J Digit Imaging 2007; 20:223–237. https://doi.org/10.1007/s10278-006-0860-9 PMID: 17021926

35. Pardoll DM, The blockade of immune checkpoints in cancer immunotherapy. Nat Rev Cancer 2012; 12:252–264. https://doi.org/10.1038/nrc3239 PMID: 22437870

36. Hahnfeldt P, Panigrahy D, Folkman J, Hlatky L, Tumor development under angiogenic signaling: a dynamical theory of tumor growth, treatment response, and postvascular dormancy. Cancer Res 1999; 59:4770–4775. PMID: 10519381

37. Perthame B, Some mathematical models of tumor growth; 2015. Universite Pierre et Marie Curie, Paris (June 2014), 23–32. Available from: https://www.ljll.math.upmc.fr/perthame/cours_M2.pdf.

38. Enderling H, Chaplain MAJ, Mathematical modeling of tumor growth and treatment. Curr Pharm Des 2014; 20:4934–4940. https://doi.org/10.2174/1381612819666131125150434 PMID: 24283955

39. Izquierdo-Kulich E, de Quesada MA, Pérez-Amor CM, Texeira ML, Nieto-Villar JM, The dynamics of tumor growth and cells pattern morphology. Math Biosci Eng 2009; 6:547–559. PMID: 19566125